

NEAR INFRARED PHOTOGRAPHY TO QUANTIFY TEMPORAL CHANGES IN MELT-FREEZE CRUSTS

Michael Smith^{1*}, Bruce Jamieson^{1,2}

¹Dept. of Civil Engineering, University of Calgary, Calgary, AB

²Dept. of Geoscience, University of Calgary, Calgary, AB

ABSTRACT: Objective quantification of snowpack stratigraphy is a difficult task, especially when multiple observers may be tracking changes over time. Properties such as grain type and size, though well defined by various snow observation guidelines, are often interpreted differently. One potential solution is the use of near infrared (NIR) photography to track the specific surface area (SSA) of a given layer. Processed images provide a quantitative measure of in-situ grain morphology free of any requirements for interpretation in the field. For the past two winters the Applied Snow and Avalanche Research Group at the University of Calgary has used NIR photography to track changes in and around buried melt-freeze crusts in the Columbia Mountains of western Canada. Eight crusts were tracked using both NIR and manual observations for periods ranging from 5 to 12 weeks. This paper describes the methods used and presents results from this study. Advantages of the method over traditional observations are also discussed, as are challenges encountered over the past two seasons.

KEYWORDS: specific surface area, crust evolution, near-infrared photography, snowpack stratigraphy

1 INTRODUCTION

Traditional snowpack observations rely on the observer's experience to record parameters such as grain type and size in a consistent manner. This may be sufficient for many applications, for instance describing the weak layer in a stability test or the failure plane of an avalanche. It is, however, impractical when small differences may be important and especially when multiple observers are involved. Because snow metamorphism is a continuous process rather than a set of discrete steps it is quite easy to miss gradual changes. In recent years the use of optical methods to quantify snowpack morphology, rather than size and shape, has seen increased use. Snow morphology influences the spectral albedo of snow (e.g. Wiscombe and Warren, 1980; Warren and Wiscombe, 1981) and has important implications in many fields of study including remote sensing (e.g. Toure et al., 2008), climate modelling (e.g. Flanner and Zender, 2006) and snow chemistry (Douglas et al., 2008).

The specific surface area (SSA) is the ratio of an element's surface area to its volume or mass. In snow the SSA typically decreases over time as dendritic forms decompose and become rounded, though Dominé et al. (2008) recorded three cases where the SSA increased over time. A variety of techniques may be used to measure the SSA: Dominé et al. (2006) used CH_4 gas absorption to measure the SSA and found a good correlation with the shortwave spectral albedo

while Gallet et al. (2009) used laser diodes to more efficiently measure the shortwave infrared reflectance of snow in the field.

Matzl and Schneebeli (2006) introduced the use of a modified digital camera to capture images in the near infrared (NIR) spectrum and employed model based stereology to determine the true SSA and derive an equation linking calibrated NIR reflectance and SSA. A number of studies since then have used similar methods to document variations in the snowpack (e.g. Langlois et al., 2010; Tape et al., 2010; Smith and Jamieson, 2009). The near infrared (NIR) is defined here as the wavelengths between the upper limit of the visible spectrum (around 750 nm) and the upper limit of sensitivity in a typical digital SLR camera, around 1100 nm.

A number of prognostic and diagnostic parametrizations of the SSA have been introduced: Taillandier et al. (2007) derived prognostic equations based on the vertical temperature gradient, while Dominé et al. (2007) proposed a parametrization based on density and grain type; Jacobi et al. (2010) introduced parametrizations from both authors into the CROCUS snow model (Brun et al., 1992) and found the best agreement with observations when using prognostic equations, though both tended to overestimate the SSA.

The use of NIR photographic methods to document changes in and around melt-freeze crusts is attractive due to their relative simplicity and the fact that they complement more traditional observations. The use of NIR offers significant advantages over images in the visible spectrum in that the penetration depth of radi-

*Corresponding author address: M. Smith, Dept. of Civil Engineering, University of Calgary, Calgary, AB, Canada; Tel 1+403-200-2904; email: ma-smith@ucalgary.ca

ation at these wavelengths is substantially less than in the visible spectrum (e.g. Wiscombe and Warren, 1980). Although it depends on a number of parameters including wavelength and grain size, and varies throughout spectrum captured by the modified camera: Gallet et al. (2009) estimates penetration depth of 3.9 cm in 200 kg/m^2 snow at 900 nm. This effectively means that the camera sensor can only 'see' what is very close to the snow surface or pit wall and is less susceptible to shallow voids or inhomogeneities.

The motivation for the focus on melt-freeze crusts is that despite observations of edge development and faceting at low temperature gradients (Dominé et al., 2003) and specifically within crusts (John Hetherington, *pers. comm.* 2009), existing parametrizations assume a decrease in SSA over time. Additionally, there are few observations of either NIR reflectance or SSA of melt-freeze crusts. This study paper presents field methods, post-processing techniques and challenges in tracking changes in the SSA of melt-freeze crusts.

2 FIELD METHODS

The goal of this study was to quantify temporal changes of the structure in and around melt-freeze crusts. Ideally something would be known about the initial structure, specifically the spatial variability, but this is in itself a difficult task (e.g. Schweizer et al., 2008). Fortunately by careful selection of study sites and by monitoring the meteorological conditions during crust formation we are able to make some assumptions about the scale of the variability: Many of the crusts tracked during this study formed over several days on uniform south-facing slopes during extended periods of high pressure. By selecting study plots with uniform sky view and which are also sheltered from the wind, many sources of variability are eliminated. For crusts that form during rain events, the spatial variability itself may be of interest; this is discussed further in Section 3.

Of five study sites, three were situated in or near Glacier National Park study plots, allowing for accurate measurement of meteorological conditions during formation. Each site was visited weekly from the time of initial burial until mid-April, at which time the snowpack was usually moist or wet. The observation wall was cut back by a minimum of 1 m from the previous week's pit and a standard test profile was recorded along with push tests (e.g. Seligman, 1936) and thermal conductivity measurements.

NIR photography field methods closely follow those described by Matzl and Schneebeli (2006); however, a brief description is included here for completeness. All photographs were taken cross-slope to reduce the risk

of contamination by adjacent layers. The pit wall was shaded by a shower curtain so that illumination was nearly diffuse. In cases where the pit wall was backlit, the snow surface was shaded at least 1.5 m back from observation wall. When possible, observations timed to coincide with periods without direct sunlight.

A metal cutting plate was used to create a smooth pit wall, ensuring that data were not influenced by scrapes or voids in the image. On warm days the pit was exposed after the camera and targets were readied in an attempt to avoid melting in the target area. Four calibration targets, made of Spectralon 50% and 99% reflectance standards, were placed surrounding the crust and 3 images were captured for averaging to correct for transient variations in illumination. A further 3 images were taken with a flat field material for later correction of variations in illumination.

The camera was a Canon D30 digital SLR camera, fitted with an 830 nm filter in front of the sensor. A manually focused 90 mm f2.8 1:1 macro lens was used for all pictures. Figure 1 shows a typical set-up, including metal frame for mounting the calibration targets. A trained observer could dig a pit, collect NIR images and record a test profile including density in approximately 90 minutes depending on target layer depth.

2.1 Challenges with field methods

A number of factors affected the quality of the data gathered in the field: Bright sunlight at the south-facing study plot created problems with overexposure of the observation wall, melting of snow and heating of instruments. Although a tripod was used for all images, a worn ball mount allowed slight movement between images and, as a result, several days did not have 3 usable images of the target area. Proper focusing was a challenge and led to a small loss of detail in some images. Finally, brittle crusts often required several attempts to create a smooth pit wall. Most challenges were easily overcome by adjusting the timing of site visits and by careful attention to methods.

3 PROCESSING AND ANALYSIS

Images were captured in either low compression JPG format or were stored directly in Canon RAW format and subsequently converted to 16 bit TIFF. The Canon D30 (like most existing digital cameras) employs Bayesian interpolation to calculate a red, green and blue intensity for each pixel on the camera's sensor. Because there are twice as many green pixels as there are red and blue, the green channel may be more desirable; however, the red channel is typically twice

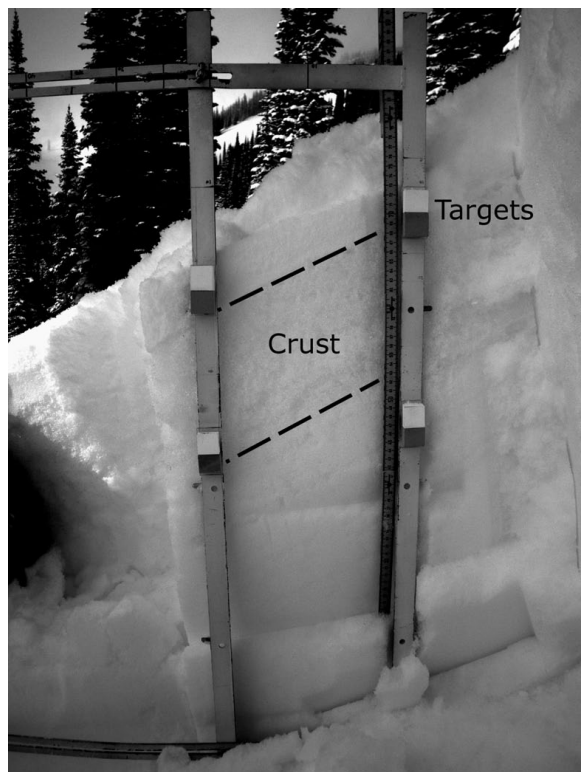


Figure 1: Typical observation wall for NIR photography. The melt freeze crust and Spectralon calibration targets are labelled.

as intense as the green and blue and was frequently the only one with sufficient illumination for further processing. Each crust was ultimately analyzed using the same channel throughout to avoid the possible introduction of variability in the results.

All processing was done using the IDL language: Its strength in dealing with large arrays and existing suite of interactive visualization tools made it ideal for this application, which requires extensive user input. Images of the crust and flat field material were averaged and a correction for lens vignetting was applied using either the flat field images or an image from an integrating sphere (see Subsec. 3.1). A dark field image corrected for repeatable noise from the camera sensor.

The calibrated NIR reflectance was obtained by deriving a linear best-fit equation from the measured intensity at the calibration targets. In all cases the R^2 value was greater than 98%. The coefficient of variation (CV) of each calibration target tracked to ensure that no contamination or pitting affected results. Although the CV was generally less than 1%, one contaminated target was identified and removed from further processing steps.

The SSA was calculated using the equation intro-

duced by Matzl and Schneebeli (2006):

$$SSA = Ae^{r/t} \quad (1)$$

Where r is the reflectance, $A = 0.017 \text{ mm}^{-1}$ and $t=12.222$ ($R^2 = 0.90$). It is useful to note that Equation 1 will introduce more variability into the processed image due to the exponential term. Figure 5 illustrates this increase as an image undergoes processing to calculate the SSA. For this reason it may be appropriate to use the calibrated NIR image for some calculations, such as the plotting of CV over time.

Each time series of SSA images was first examined for any apparent trend in morphology or variability. A region of interest (ROI) was then defined for each image, encompassing the crust as well as layers above and below it. The mean vertical profile of SSA as well as CV could then be plotted, allowing for a closer examination of trends in structure and variability. This is illustrated in Figure 2, which shows the change in SSA of a crust and layer of surface hoar over the course of a month.

By examining the vertical mean profiles of SSA and CV, we may identify more specific regions of interest (ROIs) either within the crust or at its boundaries. Based on the time series in Figure 2 it appears that the mean SSA of the crust decreases slightly along with the layer between it and the surface hoar. It also appears that both the crust and the layer below have relatively uniform vertical structures. In this case three regions were selected, consisting of the crust as well as the 2 cm layers above and below.

Summary statistics including mean, CV, standard deviation and range were generated for each ROI. There was little change in the mean vertical CV of each layer (not shown); however, there was detectable change in the mean vertical SSA: This is shown for all three regions in Figure 3. The SSA of the layer just above the crust decreases sharply while that of the crust decreases to a lesser extent. The summary values for the layer below the crust are considered unreliable due to pitting on March 15 and are not included. Due to the empirical nature of Equation 1 it is also useful to examine the ratio of the mean SSA between each ROI. Figure 4 shows the change over the same time period of the ratio between the mean SSA of the crust and that of thin layers above and below. The data reveal a large decrease of the crust SSA relative to the layer above and a variable relationship to the SSA of the layer below. Although not done here, these changes in absolute and relative mean SSA may be explored through comparison with measurements of strength, hardness and vertical temperature gradient.

Similar steps were used to analyse two crusts that

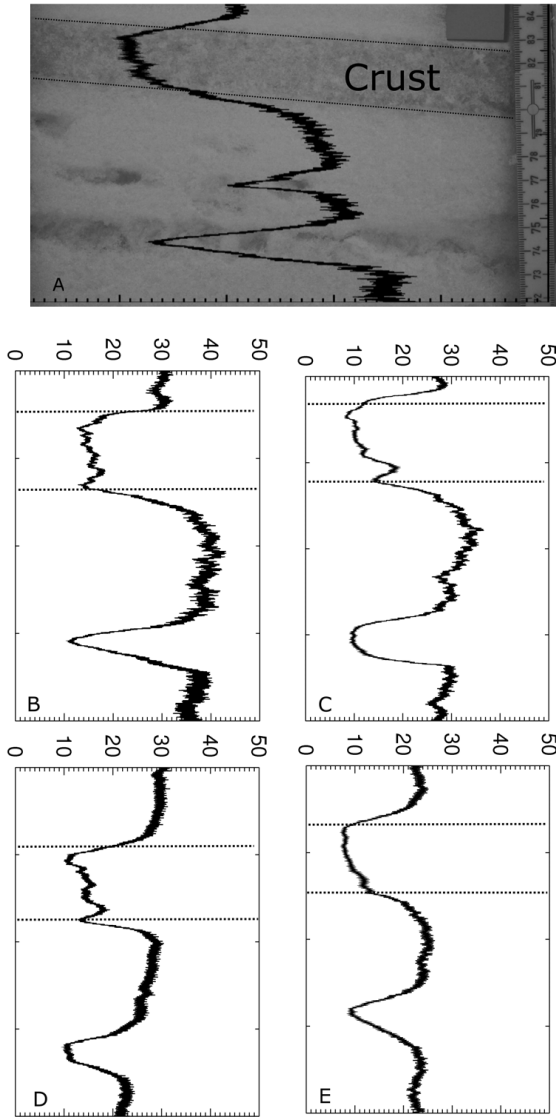


Figure 2: Weekly measurements of mean vertical SSA over one month from March 15 (A) through April 14 (E). Image A shows the SSA superimposed over an image of the crust and surface hoar. The crust is outlined by dashed lines in images B - E.

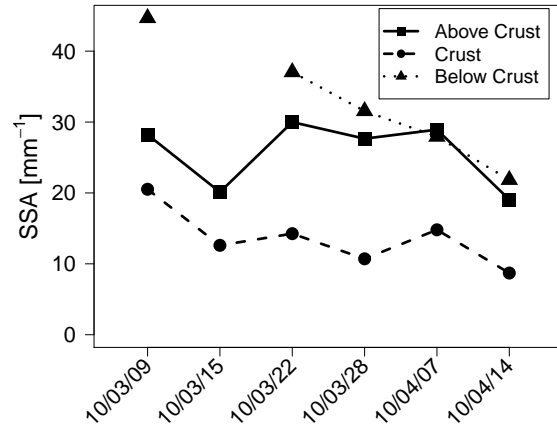


Figure 3: Change in the mean SSA of a buried crust over the course of one month. The mean value above the crust on 10/03/15 was discarded due to pitting in the wall.

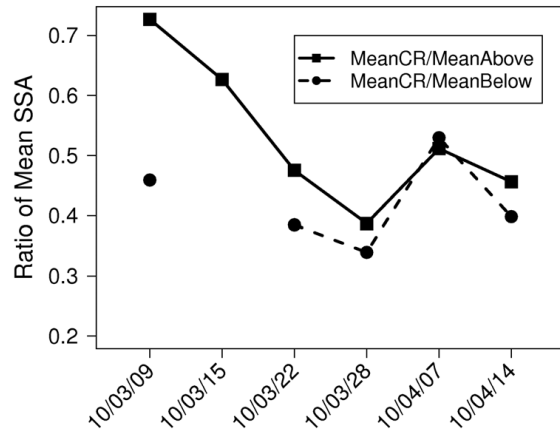


Figure 4: Change in the ratio of mean SSA of the melt-freeze crust (CR) to layers above and below.

formed during a rain event in early January 2010. In this case there was a large degree of variability at all spatial scales. Rather than focusing only on mean profiles, the horizontal variability across images was tracked over time. Though not shown here, there was an apparent trend of reduced variability as the crust underwent several melt-freeze cycles throughout the relatively warm winter of 2010.

3.1 Challenges with processing

A number of issues created problems when processing and analyzing the NIR images. Most occurred after the first field season and led to modifications of the field methods, and none of these prevented the generation of useful data. Contamination of the flat field material occurred during the first field season, and a new correction image had to be taken using an integrating

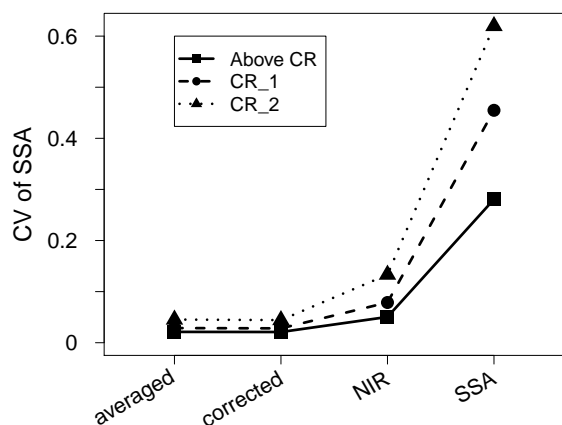


Figure 5: Increase in CV with processing of image for 3 regions of interest.

sphere. It was found that neither correction completely eliminated artefacts from the camera lens. Although quite small in magnitude relative to the overall image intensity, the artefacts are still detectable, meaning that line profiles of intensity, calibrated reflectance and SSA are prone to error. This is especially true when tracking changes through a series of images, as the lens artefacts are not constant in shape, size or intensity. A simple solution is to instead take averaged values across some horizontal extent of the image.

Equation 1 was not calibrated for images of moist or wet snow, therefore the SSA images should not be used when the layers of interest are anything but dry. The calibrated NIR images are however still valid though they should not be directly compared to images of dry snow. In this case ratios such as those in Figure 4 are appropriate.

4 SUMMARY

This paper presents a method for monitoring temporal changes in melt-freeze crusts. The same methods could equally be applied to examine spatial or temporal variability in any layer of interest. Field and analytical methods are presented along with challenges that accompany each. Analysis of a limited data set reveals a decrease in SSA of a melt-freeze crust, as well as relative changes in SSA with thin layers above and below the crust. Once trained, a single observer can easily set up and capture images in 15 minutes. Post-processing was done in IDL and a set of utilities has been created to average and correct images, select regions of interest, plot mean profiles and to calculate summary statistics. An expanded data set including both temporal and spatial data sets is presently being analyzed for inclusion in Smith (in preparation).

ACKNOWLEDGEMENTS

The authors would like to thank ASARC team members past and present. Thanks to Bruce McMahon, Jeff Goodrich and the Avalanche Control Section at Glacier National Park for ongoing logistical support and feedback. For financial support, we are grateful to the Natural Sciences and Engineering Research Council of Canada, Helicat Canada, the Canadian Avalanche Association, Mike Wiegeler Helicopter Skiing, Teck Mining Company, Canada West Ski Areas Association, the Association of Canadian Mountain Guides, Backcountry Lodges of British Columbia and the Canadian Ski Guides Association. Thanks to Backcountry Access for in-kind support.

5 REFERENCES

- Brun, E., P. David, M. Sudul, and G. Brunot, 1992: A numerical model to simulate snow-cover stratigraphy for operational avalanche forecasting. *Journal of Glaciology*, **38**, 128.
- Dominé, F., T. Lauzier, A. Cabanes, L. Legagneux, W. Kuhs, K. Techmer, and T. Heinrichs, 2003: Snow metamorphism as revealed by scanning electron microscopy. *Microscopy Research and Technique*, **62** (1), 33–48.
- Dominé, F., R. Salvatori, L. Legagneux, R. Salzano, M. Fily, and R. Casacchia, 2006: Correlation between the specific surface area and the short wave infrared (SWIR) reflectance of snow. *Cold Reg. Sci. Tech.*, **46**, 60–68.
- Dominé, F., A. Taillandier, A. Cabanes, T. Douglas, and M. Sturm, 2008: Three examples where the specific surface area of snow increased over time. *The Cryosphere Discussions*, **2** (4), 649–672.
- Dominé, F., A. Taillandier, and W. Simpson, 2007: A parameterization of the specific surface area of seasonal snow for field use and for models of snowpack evolution. *J. Geophys. Res.*, **112** (F02031).
- Douglas, T., et al., 2008: Influence of snow and ice crystal formation and accumulation on mercury deposition to the Arctic. *Environ. Sci. Technol.*, **42** (5), 1542–1551.
- Flanner, M. and C. Zender, 2006: Linking snowpack microphysics and albedo evolution. *J. Geophys. Res.*, **111** (D12208), doi:10.1029/2005JD006834.
- Gallet, J., F. Dominé, C. Zender, and G. Picard, 2009: Rapid and accurate measurement of the specific surface area of snow using infrared reflectance at 1310 and 1550 nm. *The Cryosphere Discussions*, **3** (1), 33–75.
- Jacobi, H.-W., F. Domine, W. Simpson, T. Douglas, and M. Sturm, 2010: Simulation of the specific surface area of snow using a one-dimensional physical

- snowpack model: implementation and evaluation for subarctic snow in Alaska. *The Cryosphere*, **4**, 35–51.
- Langlois, A., A. Royer, B. Montpetit, G. Picard, and L. Brucker, 2010: On the relationship between snow grain morphology and in-situ near infrared calibrated reflectance photographs. *Cold Reg. Sci. Tech.*, **61**, 34–42.
- Matzl, M. and M. Schneebeli, 2006: Measuring specific surface area of snow by near-infrared photography. *Journal of Glaciology*, **52 (179)**, 558–564.
- Schweizer, J., K. Kronholm, B. Jamieson, and K. W. Birkeland, 2008: Review of spatial variability of snowpack properties and its importance for avalanche formation. *Cold Reg. Sci. Tech.*, **51 (2-3)**, 253–272.
- Seligman, G., 1936: *Snow structure and ski fields*. Macmillan London.
- Smith, M., in preparation: Tracking changes in buried melt freeze crusts in the seasonal snowpack. Ph.D. thesis, University of Calgary.
- Smith, M. and B. Jamieson, 2009: Tracking changes in buried melt freeze crusts. *2009 International Snow Science Workshop, Davos, Switzerland, 27 September - 2 October 2009*.
- Taillandier, A., F. Dominé, W. Simpson, M. Sturm, and T. Douglas, 2007: Rate of decrease of the specific surface area of dry snow: Isothermal and temperature gradient conditions. *J. Geophys. Res.*, **112 (F03003)**, doi:10.1029/2006JF000514.
- Tape, K. D., N. Rutter, H.-P. Marshall, R. Essery, and M. Sturm, 2010: Recording microscale variations in snowpack layering using near-infrared photography. **56 (195)**, 75–80.
- Toure, A. M., K. Goïta, A. Royer, C. Mätzler, and M. Schneebeli, 2008: Near-infrared digital photography to estimate snow correlation length for microwave emission modeling. *Applied Optics*, **47 (36)**, 6723–6733.
- Warren, S. and W. Wiscombe, 1981: A model for the spectral albedo of snow. II: Snow containing atmospheric aerosols. *Journ. Atmos. Sci.*, **37 (12)**, 2734–2745.
- Wiscombe, W. and S. Warren, 1980: A model for the spectral albedo of snow. i. pure snow. *Journ. Atmos. Sci.*, **37 (12)**, 2712–2733.